A Model for the Condensation Heat Transfer of Binary Refrigerant Mixtures

Byong Joo Kim*

(*Received October 30, 1996*)

In the present work turbulent film condensation of nonazeotropic binary mixtures inside a horizontal tube is studied theoretically. The combined heat and mass transfer involved is analyzed through an integral formulation of the continuity, momentum, energy and diffusion equations. As the mass velocity of refrigerant mixtures increases, the condensation heat transfer coefficient increases. The heat transfer coefficient becomes smaller at higher mass quality. As the mole fraction of the more volatile component in binary mixtures increases, the back-diffusion mass flux of the more volatile component reduces in the vapor. As a result the condensation heat transfer coefficient improves with the increase of the inlet mole fraction of the more volatile component especially in the upstream of condenser. The results of the present study show good agreement with the experimental data available.

Key Words: Condensation Heat Transfer, Nonazeotropic Refrigerant Mixtures, Integral Analysis, Back-Diffusion Mass Flux

Nomenclature

A : Heat transfer area (m^2)
C : Mass fraction of the more volatile component in binary mixtures
D : Mass diffusion coefficients (m^2/s)
e : Internal energy (kJ/kg)
i : Enthalpy (kJ/kg)
k : Thermal conductivity (W/mK)
L : Latent heat of condensation (kJ/kg)
$\dot{m}$: Mass transfer rate (kg/s)
p : Pressure (pa)
q : Heat transfer rate (W)
r : Radial coordinates
R : Condenser radius (m)
T : Temperature (℃)
u : Velocity (m/s)
w : Mass fraction of the more volatile component in condensation flux
x : Mass quality
y : Coordinates perpendicular to flow direction
z : Axial coordinates
α : Void fraction
β : Diffusion mass transfer coefficient (m/s)
δ : Thickness (m)
μ : Viscosity (Ns/m^2)
ρ : Density (kg/m^3)
τ : Shear force (N)

Superscript

$'$: Per unit length
$''$: Per unit area

Subscript

eq : Thermodynamic equilibrium
f : Condensate film
g : Vapor
MV : The more volatile component in binary mixtures
o : Center-line value in vapor or conditions near the wall in condensate
s : Liquid-vapor interface
w : Condenser wall

* Department of Mechanical Engineering, Hongik University 72-1, Sangsudong, Mapoku, Seoul, 121-791, KOREA

1. Introduction

During past 20 years, the research work on the heat transfer of mixtures has increased for several reasons. The use of nonazeotropic refrigerant mixtures (NARM) as a working fluid could potentially improve the performance and the capacity of heat pumps and refrigeration systems by reducing the work load of compressors and the thermodynamic irreversibilities in evaporators and condensers. Also NARMs are prospective substitutes for chlorofluorocarbon (CFC) and hydrochlorofluorocarbon (HCFC) refrigerants which are considered to cause ozone depletion. Thus it is necessary to understand the mechanism of phase-change heat transfer and to predict the heat transfer and pressure drop characteristics of NARM in evaporator and condenser in addition to the thermodynamic properties.

For the case of condensation of binary vapor mixtures inside vertical tubes, several theoretical studies have been performed to analyze the heat and mass transfer mechanism. The earliest work is that of Colburn and Drew (1937) who used the Lewis-Whitman film theory and the Chilton-Colburn analogy to explain the condensation process of methanol and steam mixtures. Kotake (1978) made a theoretical investigation of laminar film condensation inside a vertical channel of variable circular cross-section. He employed the integral method for the vapor flow and the Nusselt model for the liquid film flow. The condensation heat transfer was found to be affected appreciably by the liquid-vapor equilibrium characteristics and the mass transfer process in the vapor. The flow direction had an remarkable influence on the condensation rate and film thickness. Stephan (1981) reviewed the analysis of the heat transfer with condensation in multicomponent mixtures. For the liquid film of small flow velocity compared with vapor, the Nusselt theory was proposed to be valid. Mochizuki et al. (1984) used a semi-theoretical model to predict the laminar and the turbulent film condensation in a vertical tube. Their analysis agreed well with their experiments on the binary mixtures of R11 and R114 in the laminar region but not in the turbulent region. Koyama et al. (1992) investigated the turbulent film condensation of binary mixtures inside a vertical smooth tube theoretically for the case of combined free and forced convection. Theoretical results obtained from the two layer model showed good agreement with the experiments when the values of eddy diffusivities were made lower than those in the three layer model. The effect of gravity on the wall shear stress and heat transfer was significant particularly at low vapor velocity.

Lu and Lee (1994) developed a one-dimensional analytical model for the condensation of NARM in a horizontal tube in which an annular flow pattern was assumed. It was proposed that the local diffusion flux in the liquid condensate had little effect on the local condensation mass flux. The local diffusion flux of more volatile component in the vapor (back-diffusion flux) near the liquid-vapor interface was always greater than that in the liquid (co-current diffusion flux) in magnitude.

However there are still many problems left unsolved to explain the fundamental characteristics of condensation of binary vapor mixtures fully. Furthermore the theoretical work on the condensation heat transfer of NARM in a horizontal tube is very limited.

In the present study, the turbulent film condensation of NARM inside a horizontal tube is theoretically investigated using an integral method. The results are compared with the experimental data available to verify the validity of the model. The purpose is to develop a model for better understanding the transport phenomena of the condensation heat transfer of NARM, and thus to provide the necessary information for the proper design of a condenser.

2. Formulation of the Model

Figure 1 depicts the schematic picture of condensation process in a horizontal tube and the coordinate system. As the condensation proceeds, a film of condensate forms an annular flow due to the high velocity of vapor flowing co-currently in

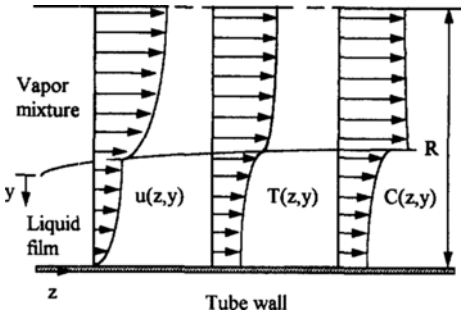

Fig. 1 Schematic picture of condensation process.

the center of tube. If a two-component mixture, whose boiling point and dew point curves are different is condensed, the component with the higher boiling point transfers preferentially into the liquid-vapor interface. In consequences, the vapor mixture at the interface contains higher concentration of the lower-boiling point, less volatile component than the vapor bulk. Figure 1 also shows the profiles of velocity, temperature, and the mass fraction of the more volatile component in both phases.

The analysis of heat transfer involving condensation of NARM includes the predictions of the local momentum, heat, and mass transfer rates and the solutions of conservation equations. Meanwhile, the constitutive relations, such as the continuity of transport variables as well as their flux at the liquid-vapor interface, are to be satisfied.

The following conditions are assumed in formulating the model.

(1) The physical properties of liquid and vapor mixture are constant and independent of temperature and mass fraction.

(2) Thermodynamic equilibrium prevails at the liquid-vapor interface.

(3) Both phases are binary mixtures of the more and the less volatile refrigerant components.

(4) The film and the vapor are turbulent flow.

(5) The film and vapor phase have fully developed velocity, temperature and mass fraction profiles.

(6) There is no slip between co-current phases.

(7) Thermal diffusion, diffusion-induced thermal effects and interdiffusion are negligible.

Under these assumptions, the integral forms of continuity, momentum, energy and diffusion (mass conservation for the more volatile component) equations in the condensate film are

$$\frac{\partial}{\partial t}\int \rho_f dA_f + \frac{\partial}{\partial z}\int \rho_f u_f dA_f = \dot{m}' \tag{1}$$

$$\begin{aligned}&\frac{\partial}{\partial t}\int \rho_f u_f dA_f - u_s \frac{\partial}{\partial t}\int \rho_f dA_f \\ &+ \frac{\partial}{\partial z}\int \rho_f u_f^2 dA_f - u_s \frac{\partial}{\partial z}\int \rho_f u_f dA_f \\ &= -\frac{\partial p}{\partial z}\int dA_f + \tau_w' - \tau_s'\end{aligned} \tag{2}$$

$$\begin{aligned}&\frac{\partial}{\partial t}\int \rho_f e_f dA_f - e_{fs}\frac{\partial}{\partial t}\int \rho_f dA_f \\ &+ \frac{\partial}{\partial z}\int \rho_f u_f i_f dA_f - i_{fs}\frac{\partial}{\partial z}\int \rho_f u_f dA_f \\ &= -q_w' + q_{fs}'\end{aligned} \tag{3}$$

$$\begin{aligned}&\frac{\partial}{\partial t}\int \rho_f C_f dA_f + \frac{\partial}{\partial z}\int \rho_f u_f C_f dA_f \\ &= \dot{m}_{MV}'\end{aligned} \tag{4}$$

where Eq. (4) is the continuity of the more volatile component of mixture in the condensate film. $\dot{m}$ is the condensation rate, q the heat transfer rate, τ the shear force, e the internal energy, and i is the enthalpy. C is the mass fraction of the more volatile component in mixtures . Subscripts f, g, s, w, and MV denote the film, the vapor, the liquid-vapor interface, the wall and the more volatile component in mixtures.

The governing equations for the vapor flow are

$$\frac{\partial}{\partial t}\int \rho_g dA_g + \frac{\partial}{\partial z}\int \rho_g u_g dA_g = -\dot{m}' \tag{5}$$

$$\begin{aligned}&\frac{\partial}{\partial t}\int \rho_g u_g dA_g - u_s \frac{\partial}{\partial t}\int \rho_g dA_g \\ &+ \frac{\partial}{\partial z}\int \rho_g u_g^2 dA_g - u_s \frac{\partial}{\partial z}\int \rho_g u_g dA_g \\ &= -\frac{\partial p}{\partial z}\int dA_g + \tau_s'\end{aligned} \tag{6}$$

$$\begin{aligned}&\frac{\partial}{\partial t}\int \rho_g e_g dA_g - e_{gs}\frac{\partial}{\partial t}\int \rho_g dA_g \\ &+ \frac{\partial}{\partial z}\int \rho_g u_g i_g dA_g - i_{gs}\frac{\partial}{\partial z}\int \rho_g u_g dA_g \\ &= -q_{gs}'\end{aligned} \tag{7}$$

$$\begin{aligned}&\frac{\partial}{\partial t}\int \rho_g C_g dA_g + \frac{\partial}{\partial z}\int \rho_g u_g C_g dA_g \\ &= \dot{m}_{MV}'\end{aligned} \tag{8}$$

Once the profiles of velocity, temperature and mass fraction are given, above equations could be transformed into differential equations. Turbulent profiles for the velocity, temperature, and the mass fraction of the more volatile component are assumed based on the one-seventh power law and the boundary conditions in the present analysis.

$$u_f(z, y) = u_s\left(1-\frac{y}{\delta_f}\right)^{1/7} \tag{9}$$

$$T_f(z, y) = T_w + (T_s - T_w)\left(1-\frac{y}{\delta_f}\right)^{1/7} \tag{10}$$

$$C_f(z, y) = C_{fs} - (C_{fs} - C_{fo})\left(\frac{y}{\delta_f}\right)^{1/7} \tag{11}$$

where δ_f is the film thickness and subscript o denotes the conditions near tube wall.

For the turbulent vapor flow, uniform-plug distributions for the velocity, temperature, and concentration profiles in the vapor phase have been adopted for simplification without affecting the model accuracy.

The liquid-vapor interfacial shear stress is given as

$$\tau_s'' = \frac{1}{2} f_s \rho_s (u_g - u_s)^2 \tag{12}$$

The friction factor at the liquid-vapor interface is correlated as (Wallis, 1969)

$$f_s = 0.079 Re_g^{-0.25}[1+75(1-\alpha)] \tag{13}$$

where α is the void fraction.

The wall shear stress is estimated similarly.

$$\tau_w'' = \frac{1}{2} f_w \rho_f \bar{u}_f^2 \tag{14}$$

where friction factor is given as

$$f_w = 0.079 Re_f^{-0.25} \tag{15}$$

The local thermal equilibrium condition at the liquid-vapor interface requires that the temperatures at both sides of the interface be equal. From assumption (2), the mass fraction of the condensate and vapor at the liquid-vapor interface should satisfy the thermodynamic equilibrium condition. The mass fraction of the more volatile component at the interface can be determined from the phase diagram for the interface temperature.

$$C_{fs} = C_{f,eq}(T_s, p) \tag{16}$$

$$C_{gs} = C_{g,eq}(T_s, p) \tag{17}$$

where p is the local pressure and eq denotes thermodynamic equilibrium.

The common characteristic of all condensation processes is the rapid decrease of the specific volume in the vapor, which results in the transport of vapor molecules to the interface. The strength of bulk transport depends on the temperature difference between the vapor and the cooling surface. Besides the gradient in the mass fraction of each component causes the diffusion mass transport in both phases. Therefore condensation mass flux is the sum of diffusion and convection flux. The continuities of heat and mass flux of the more volatile component at the liquid-vapor interface are given by

$$q_{fs}'' = \dot{m}'' L + h_{gs}(T_g - T_s) \tag{18}$$

$$C_{fs}\dot{m}'' + \beta_f \rho_f (C_{fs} - \bar{C}_f) = C_{gs}\dot{m}'' + \beta_g \rho_g (C_g - C_{gs}) \tag{19}$$

Here β is the diffusion mass transfer coefficient. Coefficients for heat and diffusion mass transfer in the vapor can be evaluated from the analogies among mass, momentum and energy transfer. The diffusion mass transfer coefficient in the condensate film is calculated based on the film thickness, the mass diffusivity of liquid mixtures and the mass transfer enhancement factor, C_m.

$$\beta_f = \frac{C_m \rho_f D_f}{\delta_f} \tag{20}$$

For the condensate film of wavy-turbulent motion, the mass transfer enhancement factor can be estimated from the ratio between the film thickness and the thickness of the laminar sublayer near the liquid-vapor interface.

3. Solution Method

Due to the nonlinear nature of the conservation equations and constitutive relations, it is difficult to solve them simultaneously. Therefore, a model is formulated with transient equations and the initial conditions are assumed to be those of the inlet boundary conditions. Then the equations are solved until the rate of change of any variable with respect to time is negligible, at which steady state is assumed to be reached.

Equations (1)~(8), (16), (17) and (19) form 11 simultaneous equations for the unknowns of δ_f, u_s, u_g, T_s, T_g, C_{fs}, C_{fo}, C_{gs}, C_g, $\dot{m}''$ and p. They are solved by the explicit finite difference method. Discretization of equations using the first-order forward-time and backward-space scheme results in the difference equations. The temperature and the mass fraction of the more volatile component in mixtures are strongly coupled by the thermodynamic equilibrium conditions at the liquid-vapor interface. At the same time they should meet the continuity requirements at the liquid-vapor interface as given in Eqs. (18) and (19).

At each time step, calculation proceeds from the inlet to the outlet of the condenser. At each node, the condensate film thickness is first calculated from Eq. (1), and then the interfacial velocity, the vapor core velocity and the pressure are calculated by Eqs. (2), (5) and (6). The temperature and the mass fraction of the more volatile component in condensate film and vapor are calculated from the energy and diffusion equations for both phases with the interfacial conditions of Eqs. (16), (17) and (19).

For an analysis of heat transfer in turbulent condensation process, the inlet conditions should be provided as boundary conditions. Basically the total mass flowrate and the system pressure are selected based on the practical operating conditions of refrigeration system. Since the present analysis is limited for the turbulent condensate film, the film Reynolds number at the inlet of solution domain is assumed to be the transition Reynolds number for the annular film flow, which is around 1000. Therefore the condensate flowrate could be estimated. Once the condensate and vapor flowrate are known the film thickness and the mean velocity of condensate film and vapor could be calculated based on the mass continuity and the momentum balance for both phases.

4. Results and Discussion

The model developed is applied to the condensation heat transfer with R22 and R114 mixtures in a horizontal tube. Due to the limited experimental data available, the operating conditions for a condenser are adopted from those of Koyama et al. (1994) for the later comparison and verification. Table 1 shows the boundary and operating conditions of condensation process of R22 and R114 mixtures. The coolant flows counter-currently with the vapor in the annulus of a double-pipe type condenser.

Table 1 Base-line conditions and the range of parameters for the analysis of condensation process.

Parameters	Base-line values	Ranges
Mixture components	R22 and R114	
Condenser inner diameter (m)	0.0079	
Condenser length (m)	5.0	5.0-6.0
System pressure (bar)	12.2	10.8-12.2
NARM mole fraction (%)	50.0	25.0-75.0
NARM inlet superheating (℃)	0.0	
NARM mass velocity (kg/m²s)	170.0	170.0-283.0
Coolant inlet temperature (℃)	24.0	
Coolant flowrate (kg/s)	0.01	0.01-0.02

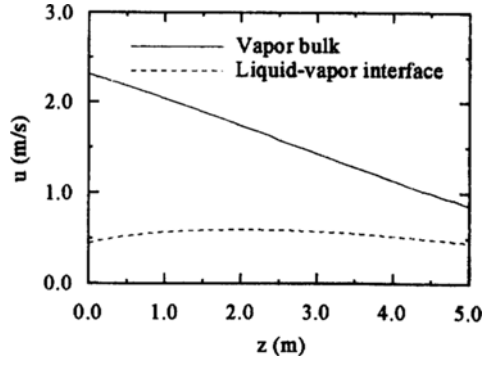

Fig. 2 Variation of velocity along the condenser.

Figure 2 shows the variation of the liquid-vapor interface velocity and the vapor bulk velocity along a horizontal condenser. Since the vapor mixture flows at high velocity near inlet,

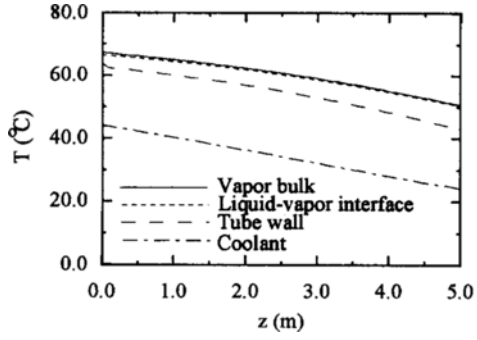

Fig. 3 Variation of temperature along the condenser.

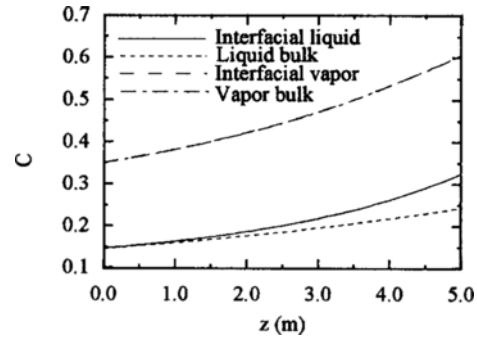

Fig. 4 Variation of mass fraction of the more volatile component along the condenser.

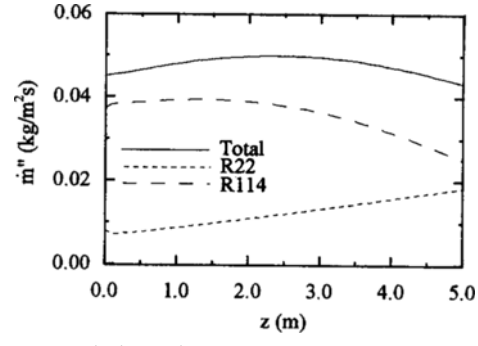

Fig. 5 Variation of condensation fluxes along the condenser.

appreciable interfacial shear stress develops at the liquid-vapor interface. Even though the annular condensate film gets thicker as the vapor condenses at the liquid-vapor interface, the interfacial velocity increases particularly in the upstream of condenser. However the liquid-vapor interfacial velocity decreases with the mass velocity of the vapor and the film thickness increases in the downstream of condenser.

For the NARM vapor, condensation occurs when the wall temperature is lower than its dew point. The interfacial temperature depends on the local thermal boundary conditions and lies between the dew point and the bubble point. Since the wall temperature is less than the interfacial temperature, the bulk average temperature of the condensate must fall below the interfacial temperature. The temperature variation of vapor bulk, liquid-vapor interface, condenser wall, and coolant are given in Fig. 3. Due to the coolant of low temperature flowing counter-currently, condenser wall temperature is lower than that of the vapor bulk. Their temperature difference remains almost the same along the condenser. The vapor bulk temperature decreases continuously along the condenser and is slightly higher than the interfacial temperature, which is the dew point for the interfacial vapor and bubble point for interfacial liquid. The coolant temperature seems to increase almost linearly, which suggests the condensation flux does not vary very much along the condenser.

The variations of the mass fraction of interfacial liquid, liquid bulk, interfacial vapor, and vapor bulk along the condenser are plotted in Fig. 4. Flowing downstream in the condenser, the mass fraction of the condensate is smaller than that of the interfacial vapor. The bulk average mass fraction of the condensate is always less than the interfacial liquid. For the condensate to gain the bulk mass fraction close to the value of the vapor at the inlet of condenser, the mass fraction of the interfacial liquid should be greater than that of inlet vapor. Meanwhile, the mass fraction of the vapor is raised to the value of the pure light component, which will approach unity after complete condensation. The difference of mass fraction between the vapor bulk and the interfacial vapor seems to be negligibly small due to the high diffusion mass transfer coefficient in the vapor side. However the mass fraction of the interfacial vapor is always higher than that of the vapor bulk.

The condensation flux of NARM is the sum of the more volatile and the less volatile component,

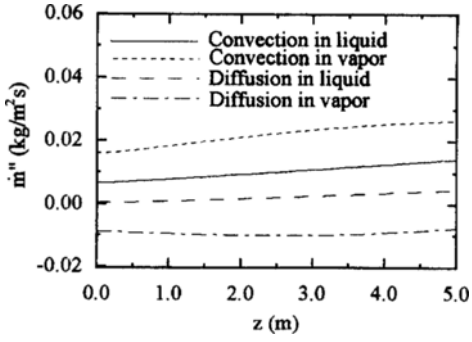

Fig. 6 Variation of diffusion and convection mass flux of R22 along the condenser.

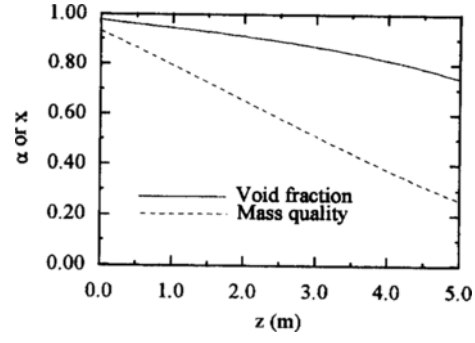

Fig. 7 Variation of void fraction and mass quality along the condenser.

which are R22 and R114 respectively in the present study. Figure 5 shows the variation of total condensation flux and the contribution of each component. Even though the total condensation flux seems to be insensitive to the local condition, the condensation flux of each component varies very much along the condenser. As the wall temperature decreases and the mass fraction of the interfacial liquid increases, the condensation flux of the more volatile component, R22, increases consistently along the condenser. While the less volatile component, R114, shows higher condensation flux in the upstream than in the downstream of the condenser.

The condensation flux of each component consists of the diffusion and the convection mass flux. For both phases the transport of the more volatile component is resulted mainly by the bulk motion as shown in Fig. 6. This convectional transport is stronger in the vapor side. Since the temperature at the interface is always less than the temperature of the axial vapor flow, the mass fraction of the interfacial vapor is always greater than the mass fraction of the vapor bulk. A back-diffusion flux of the more volatile component from the interface to the vapor bulk flow then occurs. This back-diffusion retards the mass diffusion from the vapor core to the interface and results in a reduction of the local condensed mass flux and thus the heat transfer rate. On the other hand, the mass fraction of the interfacial liquid is greater than that of the bulk condensate flow. The more volatile component in the condensate film therefore diffuses from the interface toward the inner wall (co-current diffusion flux). For the turbulent flow of the vapor, the mass transfer coefficient is so great that the magnitude of the back-diffusion is bigger than that of the co-current diffusion flux in the condensate film. However, near the outlet of the condenser where the vapor velocity should be very small, the back-diffusion flux seems to vanish while the co-current diffusion flux in the condensate film increases monotonously.

As the vapor condenses at the liquid-vapor interface, the mass quality and the void fraction varies as shown in Fig. 7. Since the temperature difference between the condenser wall and the coolant remains almost constant, the mass quality of NARM decreases linearly with the condenser length. However the decrease of void fraction is small due to relatively high velocity of the condensate film except near the outlet of the condenser. Based on the variation of void fraction along the condenser, it can be easily understood that the growth of the condensate film thickness becomes noticeable near the end of the condenser.

As the condensation proceeds, the mass quality decreases with increasing condensate film thickness. The thickness of the condensate film governs the heat transfer resistance. While the temperature profile in the condensate film determines the driving temperature difference. Generally the condensation heat transfer coefficient decreases as the mass quality decreases. However the heat transfer coefficient near the inlet of the condenser shows the reduced slope since the growth of condensate film thickness is retarded due to the high interfacial shear stress. In the downstream of the

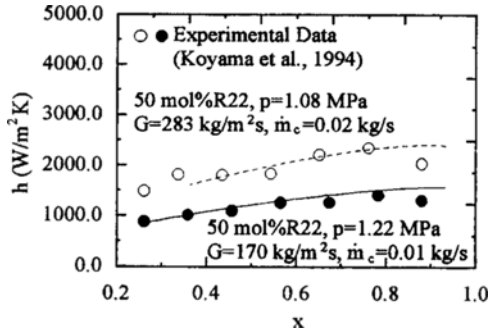

Fig. 8 Comparison of the predicted condensation heat transfer coefficient with experimental data.

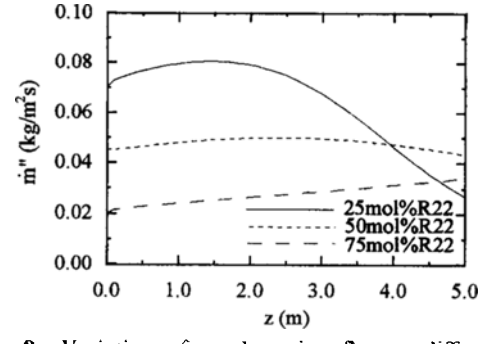

Fig. 9 Variation of condensation flux at different mole fractions of R22.

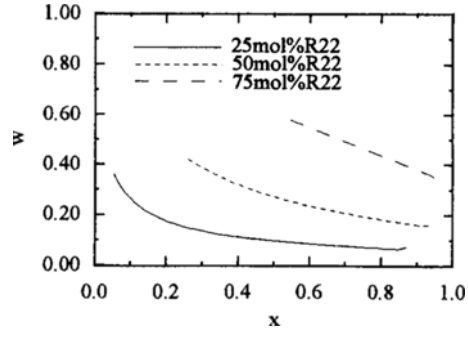

Fig. 10 Effects of an inlet mole fraction of R22 on the mass fraction of R22 to the total condensation flux.

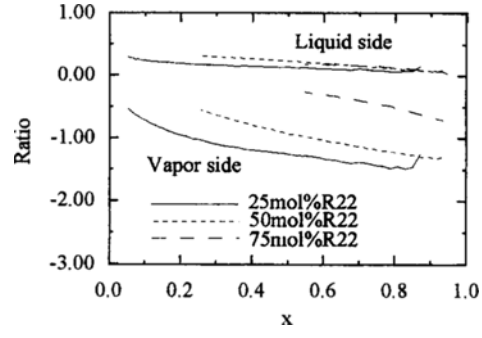

Fig. 11 Ratio of diffusion mass flux to condensation mass flux of R22 as a function of the mass quality.

condenser, the heat transfer coefficients shows rapid decrease with the reduction in the mass quality. Figure 8 shows the comparison of the present work with the experimental data (Koyama et al., 1994). The condensation heat transfer coefficients for two different operating conditions, but at the same inlet mole fraction of the more volatile component in mixtures, are compared as a function of the mass quality. Within the range of analysis, they shows good agreement. It verifies the reliability of the present model for the condensation heat transfer with NARM.

As the mole fraction of the more volatile component increases, the dew and the bubble points of binary mixtures decrease. The latent heat of evaporation for the mixtures of R22 and R114 increases with the mole fraction of the more volatile component. Consequently The condensation flux decreases substantially with the inlet mole fraction of the more volatile component, R22, as shown in Fig. 9. It also shows the decrease of the condensation flux as the mass quality increases in the downstream of the condenser.

Since the mass fraction of the interfacial liquid and vapor increases along the condenser, the gradient of mass fraction profile in the condensate film and vapor bulk develops. Thus the mass fraction of the more volatile component in total condensation flux, w, varies with the condenser length

$$w=\frac{\dot{m}''_{R22}}{\dot{m}''_{R22}+\dot{m}''_{R114}} \tag{21}$$

The mass fraction of the R22 in the total condensation flux increases with the increase of the mole fraction of R22 at the inlet condenser as shown in Fig. 10. Basically the mass fraction of R22 in total condensation flux increases with the

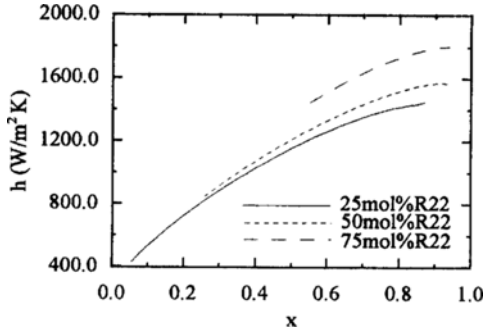

Fig. 12 Effects of an inlet mole fraction of R22 on condensation heat transfer coefficient.

condenser length, where the mass quality decreases. The increase of mass fraction of R22 in condensation flux is more rapid at lower mass quality since the mass fraction of R22 in the vapor bulk decreases.

The contributions of diffusion mass flux of R22, in terms of the ratio of diffusion mass flux to condensation mass flux of R22, in the vapor and condensate film are given in Fig. 11. The negative value in the vapor bulk means the back-diffusion flux, which retards the mass transfer from the vapor to the interface and results in a reduction of the local condensation mass flux as well as the heat transfer rate. The positive ratio in the condensate film is the result of the co-current diffusion flux of the more volatile component from the interface to the liquid bulk. In the upstream of condenser, as proposed by Lu and Lee (1994), the influence of the back-diffusion flux in the vapor is far stronger than that of the co-current diffusion flux in the condensate film because the convection strength on the vapor side is stronger and the concentration gradient in the condensate film is small. In the downstream of the condenser, the mass fractions of interfacial vapor and liquid, as well as the vapor, approach unity. The back -diffusion flux vanishes and the strength of the co -current diffusion flux will becomes stronger.

The condensation heat transfer coefficient as a function of the mass quality at the different inlet mole fraction of R22 is shown in Fig. 12. The qualitative characteristics of the heat transfer coefficient are similar regardless of the mole fraction of R22. The reduction rate of heat transfer coefficient increases as the mass quality decreases. At higher inlet mole fraction of R22, the condensation heat transfer coefficient is higher especially at higher mass quality. It might be the result of the reduced back-diffusion flux in the vapor at the high inlet mole fraction of the more volatile component as explained in Fig. 11. However, at lower mass quality, the condensation heat transfer coefficient seems to come up with almost the same values, which agrees well with the experimental findings (Koyama et al., 1994).

5. Conclusions

In the present work turbulent film condensation of nonazeotropic binary mixtures inside a horizontal tube is studied theoretically. An integral approach is used for the mathematical formulation of the governing equations for both phases. They are solved with the constitutive relations at the liquid-vapor interface.

As the mass flux increases, the condensation heat transfer coefficient increases. The heat transfer coefficient becomes smaller at higher mass quality. The results of the present study shows good agreement with the experimental data available. As the mole fraction of the more volatile component in binary mixtures increases, the back -diffusion mass flux of the more volatile component decreases in the vapor. While the co-current diffusion mass flux in the condensate film does not seem to be affected very much. As a result the condensation heat transfer coefficient increases as the inlet mole fraction of the more volatile component increases especially in the upstream of the condenser.

Acknowledgment

This work was supported by the AFERC of POSTECH; the financial assistance is gratefully acknowledged.

References

Colburn, A. P., Drew, T. B., 1937, "The Condensation of Mixed Vapors," *Trans. Am. Inst.*

Chem. Engng, Vol. 33, pp. 197~215.

Kotake, S., 1978, "Film Condensation of Binary Mixture Flow in a Vertical Channel," *Int. J. Heat Mass Transfer*, Vol. 21, pp. 875~884.

Koyama, S., Dilao, C. O., Fujii, T., 1992, "Turbulent Film Condensation of Binary Mixtures inside a Vertical Tube," *Proc. 2nd JSME-KSME Thermal Engineering Conf.*, Vol. 2, pp. 427~432.

Koyama, S., Dilao, C. O., Fujii, T., 1994, "Condensation Heat Transfer of Refrigerant Mixtures inside Horizontal Tubes," *Proc. of WTPF*, pp. 175~190, AFERC, POSTECH.

Lu, D. C., Lee, C. C., 1994, "An Analytical Model of Condensation Heat Transfer of Non-azeotropic Refrigerant Mixtures in a Horizontal Tube," *ASHRAE Summer Meeting*, OR-94-7-3, Orlando.

Mochizuki, S., Yagi, Y., Tadano, R., Yang, W. J., 1984, "Convective Filmwise Condensation of Nonazeotropic Binary Mixtures in a Vertical Tube," *Trans. ASME, J. Heat Transfer*, Vol. 106, pp. 531~538.

Stephan, K., 1981, "Heat Transfer with Condensation in Multicomponent Mixtures," in *Heat Exchangers-Thermal-Hydraulic Fundamentals*, Edited by Kakac, S., Bergles, A. E., Mayinger, F., McGraw-Hill.

Wallis, G. B., 1969, *One Dimensional Two Phase Flow*, Mc-Graw Hill.